# Scanning Tunneling Luminescence of Individual CdSe Nanowires

*Theresa Lutz,\* Alexander Kabakchiev, Thomas Dufaux, Christian Wolpert, Zhe Wang, Marko Burghard, Klaus Kuhnke, and Klaus Kern*

*The local luminescence properties of individual CdSe nanowires composed of segments of zinc blende and wurtzite crystal structures are investigated by low-temperature scanning tunneling luminescence spectroscopy. Light emission from the wires is achieved by the direct injection of holes and electrons, without the need for coupling to tip-induced plasmons in the underlying metal substrate. The photon energy is found to increase with decreasing wire diameter due to exciton confinement. The bulk bandgap extrapolated from the energy versus diameter dependence is consistent with photon emission from the zinc blende-type CdSe sections.*

## 1. Introduction

Semiconductor nanostructures exhibit an excellent tunability of their electronic and optical properties by the variation of their size, shape, composition, and lattice structure. This property makes them valuable building blocks for electronic and photonic devices such as lasers or light-emitting diodes.[1] The successful implementation of light-emitting nanostructures requires a detailed understanding of their charge-transport properties, as well as the electron–hole pair creation and photon generation processes involved. To this end, local probing of individual semiconductor nanostructures, with the aim of identifying the influence of impurities, defects, and different crystal lattice structures, has gained increasing importance. One useful experimental approach is scanning tunneling luminescence (STL), which involves the detection of local photon emission induced by the injection of charge carriers from the tip of a scanning tunneling microscope (STM). This technique furthermore provides combined topographic and spectroscopic information on the atomic scale.[2]

STL studies have been intensively performed on the luminescence in III/V semiconductor heterostructures, wherein quantum wells,[3–5] quantum wires[6,7] or quantum dots[8–10] are embedded in a larger-bandgap material to achieve carrier confinement. In contrast, there are only a few reports on STM-induced light emission from freestanding semiconductor nanostructures deposited on a metal substrate.[11–13] In these studies on CdSe/ZnS core/shell quantum dots, the light emission couples to plasmons excited by the tunnel current in the underlying metal substrate. However, since the existence and the spectral intensity of tip-induced plasmons strongly depend on the shape and composition of the tip and the substrate, it is rather difficult to control this type of emission.[14,15] Herein, we report on the STM-induced excitation of luminescence in individual CdSe nanowires (NWs; see **Figure 1**a), for which the light emission does not rely on the simultaneous stimulation of tip-induced plasmons. Instead, tunneling-induced luminescence is enabled by ensuring an intimate electronic coupling between the NWs and the gold substrate, such that charge injection into the wires can easily occur. Laterally resolved luminescence spectra and light-intensity maps in combination with topographic information allow us to probe the local optical properties of CdSe NWs, and to identify the origin of the light emission.

Dr. T. Lutz, Dr. A. Kabakchiev, T. Dufaux, C. Wolpert, Dr. M. Burghard, Dr. K. Kuhnke, Prof. K. Kern
Max-Planck-Institute for Solid State Research
Heisenbergstr. 1, 70569 Stuttgart, Germany
E-mail: t.lutz@fkf.mpg.de

Z. Wang
Institute of Physical Chemistry
University of Hamburg
Grindelallee 117, 20146 Hamburg, Germany

Prof. K. Kern
Institute de Physique de la Matière Condensée
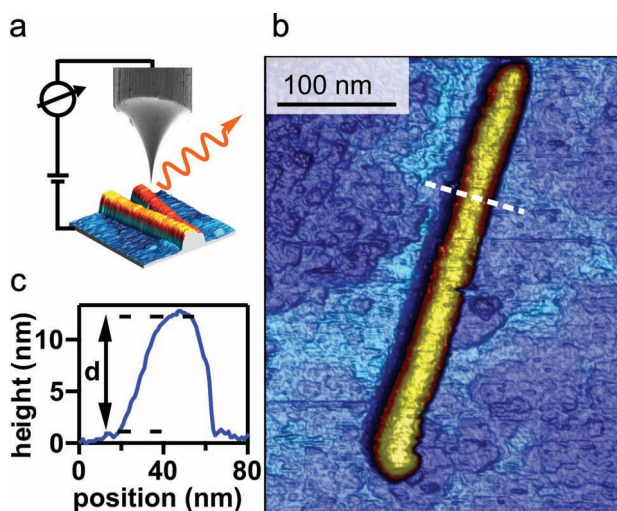Ecole Polytechnique Fédérale de Lausanne
1015 Lausanne, Switzerland

**Figure 1.** a) Schematic illustration of the experimental setup for STL detection. b) Constant-current STM image of a CdSe NW. c) Height profile along the dashed line in (b).

## 2. Results and Discussion

### 2.1. Local Light Emission and Luminescence Peak Shape

CdSe NWs, grown by the solution–liquid–solid (SLS) method, were deposited onto a gold substrate under ambient conditions. According to transmission electron microscopy (TEM) and X-ray analysis, the obtained single-crystalline CdSe wires consist of alternating zinc blende (3–6%) and wurtzite structural units, which lead to a local variation of the band structure of the NWs.[16] The NWs are capped with tri-octylphosphine oxide (TOPO), which renders them soluble and passivates their surface. The samples were transferred into an ultrahigh-vacuum (UHV) chamber. After annealing at 420 K for 5 min to remove contaminants (e.g., water), the sample was transferred into a home-built STM equipped with a liquid He cryostat held at 4.2 K. A photon detection unit was integrated in the STM to collect photons which originated from the tunneling junction.[17] Complementary to the STM investigations, photoluminescence (PL) measurements were performed at 12 K.

A typical STM image of an individual CdSe NW is displayed in Figure 1b together with the corresponding height profile in Figure 1c. While the measured height of the wires is reliable within the limits of surface roughness, the apparent wire width is strongly increased due to the convolution of NW and tip shape, as exemplified by the width of ≈40 nm determined for the approximately 12-nm-thick CdSe wire in Figure 1b. Atomic resolution of the NWs could not be achieved, most likely due to residuals of the capping ligands that could not be removed during sample annealing, as well as other contaminants originating from the sample preparation under ambient conditions. STL could be detected from individual NWs upon applying tunneling currents between 1 and 3 nA and bias voltages between –2 and –4 V (the tip potential is defined as 0 V). Light emission occurred exclusively in

the negative-bias range, which corresponded to the injection of holes from the STM tip into the sample.

Although the emission could be reproducibly observed on some NW sections, others remained completely dark even for higher applied voltages. This is exemplified in **Figure 2**, in which an STM image of a NW section (Figure 2a) is compared with the corresponding photon map (Figure 2b). Like in Figure 1b, the convolution of the NW and the STM tip causes the NW to appear much broader (≈100 nm) than its nominal width (≈20 nm), such that the NW fills the whole image in Figure 2. The comparison of the topography with the photon map shows that some small regions (one is marked by a rectangle) on the NW show a higher conductivity (i.e., they appear bright yellow), which might originate from slight tip modifications. However, the appearance of the more extended luminescent regions (indicated by an ellipse) is independent of tip modifications and is well reproducible for repeated image scans, thereby revealing that light emission is a local property of the NW. The reason for this observation will be discussed below.

**Figure 3**a depicts STL spectra recorded on three NWs with different diameters, which exhibit a prominent peak around 1.8 eV. In each case, no other luminescence features could be observed (in the detection range of 1.5 to 3.5 eV), including surface plasmons of the gold substrate which would emerge as a broad feature from approximately 1.4 to 2.5 eV.[18] The absence of plasmon coupling in our experiments is different from most other STL measurements on freestanding nanoscale objects.[11–13] The assignment of the luminescence peaks to the NWs gains support from their close similarity to the PL spectrum in Figure 3b. In particular, comparison of the PL spectrum with the STL spectrum of the 18 nm wire reveals almost identical peak shape and width. This characteristic distinguishes the present STL spectra from electroluminescence (EL) spectra of single CdSe NWs[19,20] that display much
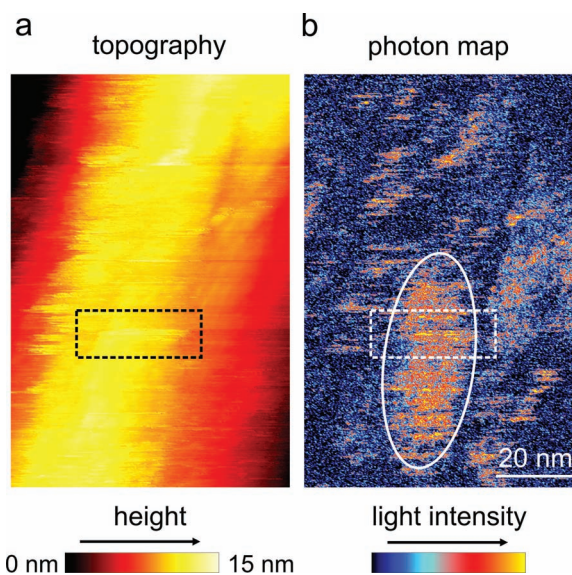


**Figure 2.** a) STM image of a NW and b) the corresponding photon map (tunneling parameters: 1.5 nA, –3.5 V). The rectangles and the ellipse are explained in the main text.
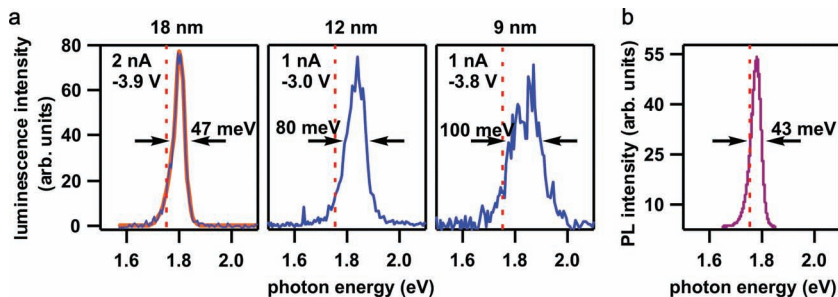
**Figure 3.** a) STL spectra for NWs of three different diameters: 18, 12, and 9 nm (orange line: sum of two Gaussian functions). b) PL spectrum at 4 K. The dotted vertical lines mark the extrapolated bulk exciton energy of zinc blende-type CdSe (see Figure 4).

broader emission peaks associated with surface states introduced during device fabrication. There is no definite evidence that the PL spectrum in Figure 3b originates from a single wire, although the position of the laser spot (500 nm in diameter) was carefully chosen. However, the local charge injection in STL allows the STL spectrum to be attributed to the local emission from an individual wire.

In Figure 3a it can be seen that the spectral peak is asymmetric and that its energy depends sensitively on the wire diameter. In general, the peak can be well fitted by a sum of two Gaussian functions, as demonstrated for the spectrum of the 18 nm wire in Figure 3a. Of these two components, the shoulder on the low-energy side of the main peak can be attributed to exciton–phonon coupling, mediated by the longitudinal optical (LO) phonon with an energy of 26 meV.[21] Some spectra clearly show the presence of two peaks separated by a few tens of meV, as demonstrated for the 9 nm wire in Figure 3a. This observation might be explained by the corrugation of the electronic potential along the NW axis caused by alternating zinc blende and wurtzite sections, which leads to a "type II" band alignment. In agreement with our experimental observations, the energy difference between the direct transition in the zinc blende-type structure and the indirect transition at the intersection of zinc blende and wurtzite regions is of the order of 50 meV.[22] It should be mentioned that the broad emission linewidths of the STL peaks (≈50–100 meV) have also been observed in several previous studies on semiconductor NWs. They were attributed to fluctuations in the dielectric contrast (caused, e.g., by inhomogeneity in the TOPO passivation), the presence of radiative surface states, or small-diameter variations.[22,23]

## 2.2. Diameter Dependence of the Emission Peak

Recent studies have revealed that the bandgap of semiconductor NWs does not scale exactly with the inverse square-diameter as expected from the simple particle-in-a-box model. Instead, the bandgap of CdSe NWs follows a diameter dependence, $d^{-1.36}$.[24,25] This dependence also accounts very well for the higher-energy peak component in the present spectra, as demonstrated by the plot in **Figure 4** where the red line represents the least-squares linear fit to the data, from which an emission peak minimum in the bulk limit $d \rightarrow \infty$ of $E_{gap}^{bulk} \approx 1.75$ eV is derived. This result is in excellent

agreement with the free exciton energy reported for CdSe zinc blende crystals at 4 K.[21] In comparison, the exciton energy of wurtzite-type CdSe crystals is considerably larger by 80 meV (≈1.83 eV).[21] Accordingly, we attribute the segments that lack light emission to wurtzite-type CdSe segments. It should be emphasized that the photon map in Figure 2 displays the regions where charge injection leads to radiative recombination, which can also occur after diffusion and thermalization of the injected charge carriers. Hence, even if charge carriers are injected into a wurtzite structure, they can diffuse a few tens of nanometers[26] and recombine radiatively if a zinc blende region lies within the diffusion path. This most likely explains why the light-emitting regions in Figure 2b are wider (up to ≈50 nm) than the typical length of zinc blende regions (a few nanometers). The optical inactivity of the wurtzite-type sections will be rationalized below.

It is furthermore worthwhile comparing the fitted slope of the diameter dependence to literature values.[24] According to both theory and experiments, the slope reflects the dimensionality of the system,[27] and its magnitude decreases with increasing dimensionality. The present slope of 2.6 eV nm$^{1.36}$ is larger than the value of 1.8 eV nm$^{1.36}$ documented in Reference [24] for CdSe NWs, which suggests that quantum-dot-like zinc blende segments are responsible for the light emission. This assertion is in accord with the small length of these segments of a few nanometers, as observed by TEM.[16] Nonetheless, in Figure 4 we have used the exponent of 1.36 established for NWs, since previous studies on similar systems have revealed only a small difference between the exponents for the zero- and the one-dimensional cases.[27] For the preceding analysis, we have assumed that the energy shift due to the finite length of the zinc blende regions is less pronounced than the shift due to the lateral confinement by the wire diameter. This procedure is reasonable since the interface to an adjacent wurtzite region
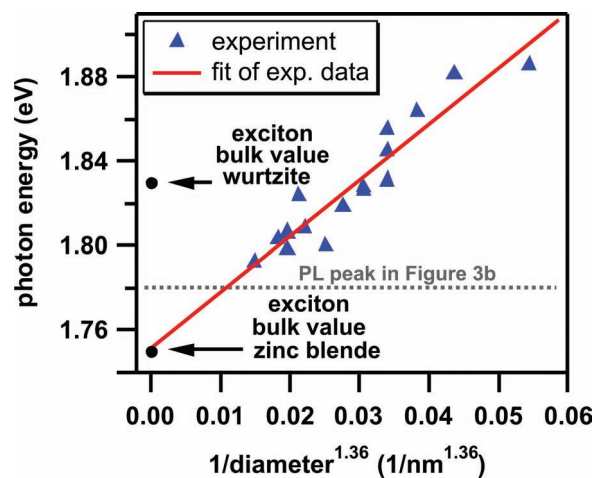


**Figure 4.** Photon energy as a function of the diameter, $d^{-1.36}$. The gray dotted line shows the energy of the PL peak of Figure 2b, which can be related to a NW with larger diameter (approximately 20 nm).

imposes less rigorous boundary conditions to the excitons than the NW surface. However, any scatter of the length of zinc blende segments in the measured NWs will contribute to the vertical scatter of the data in Figure 4. Another contribution might arise from possible spatial variations of the TOPO coverage, which modifies the dielectric surroundings and thus the exciton binding energy.[22] Consistent with the latter assumption, we have observed small variations ($\approx$20 meV) in the energy of the emission spectra along the NWs.



**Figure 5.** a) Integrated luminescence intensity as a function of sample voltage. b) Schematic model of the excitation mechanism; $E_{F,Au}$, $E_{F,W}$, and $E_{F,CdSe}$ are the Fermi levels of the Au substrate, the W tip, and the CdSe NW, respectively. The conduction and valence bands of wurtzite and zinc blende-type CdSe are indicated by the dashed and solid lines, respectively. c) Schematic of the zinc blende- and wurtzite-type band structure in the direction parallel to the CdSe NW.

### 2.3. Light Excitation Mechanism

Regarding the mechanism underlying the STL generation from the NWs, the coupling of metal plasmon modes to the wires[12,13] can be ruled out, since we do not observe plasmonic emission on the gold substrate before and after the luminescence measurements. This finding is in agreement with previous studies, which found reduced plasmonic emission for tungsten tips as compared to, for example, Au, Ag, or PtIr tips.[28,29] A further suppression of the emission may arise from surface contaminants resulting from the sample preparation under ambient conditions.[30] Moreover, even if plasmons could be excited, their coupling to excitons in the NWs is unlikely, since the electric field of the plasmon (perpendicular to the substrate) is perpendicular to the transition dipole of the NW (parallel to the wire axis).[31] Likewise, impact ionization is unlikely to play a role, as this process usually sets in at voltages much larger than 2 V, and is furthermore polarity-independent.[32,33] By contrast, all the STL characteristics observed in our experiments can be consistently explained by carrier injection from both the gold substrate and the STM tip.

Light emission from the NWs occurs only in the negative-bias range for voltages below approximately –2 V (see **Figure 5**a), that is, for voltages exceeding the photon emission energy by more than 0.2 eV. In the positive-bias range, no luminescence could be detected even for voltages as high as +10 V. This asymmetry can be understood by the presence of n-doped CdSe wires, the Fermi level of which is pinned to the gold substrate such that hole injection is attainable only from the tungsten tip (Figure 5b). The n-type doping of CdSe is well documented, for example, for thin evaporated films of CdSe[34–36] with electron concentrations of up to $10^{18}$ cm$^{-3}$. In addition, electrical transport measurements on single CdSe NWs have clearly revealed n-type behavior.[20] In our experiments, n-doping may be further promoted by sample annealing under UHV conditions, whereupon selenium vacancies are likely to be introduced into the NW.[37] At the same time, the annealing is expected to partially remove the TOPO molecules on the NWs and thus to promote the Fermi-level pinning, which requires an intimate electronic coupling between wire and gold substrate. In the scenario of Figure 5b, electrons would tunnel from the gold substrate into the conduction band of the NW, from where they recombine with holes injected from the
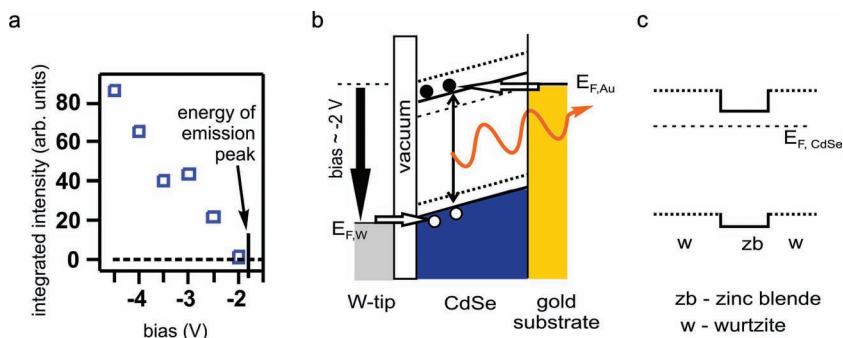
tip. Such a mechanism could explain why the light emission is restricted to the zinc blende sections, as its conduction-band edge lies approximately 100 meV below that of the wurtzite phase (Figure 5c),[22] and hence electron injection from the substrate into the latter sections might be suppressed due to the above-mentioned Fermi-level pinning. This assumption gains further support from a recent theoretical study of Zhang et al.,[38] which indicates that for small InP NWs a type II to type I band alignment transition takes place, thereby leading to an accumulation of holes as well as electrons in the zinc blende-type segments. A similar transition might also occur in the case of the present CdSe NWs. Another contributing factor could be the strong permanent dipole inherent to the wurtzite sections, which is aligned along the NW axis.[39–41] This dipole may induce a spatial separation of the injected charge carriers, thus preventing their radiative recombination. Additionally, light emission might be inhibited in both types of lattice structure by local nonradiative recombination of charge carriers via defect sites deep in the bandgap.[42]

## 3. Conclusion

In summary, we have demonstrated that STL enables local light generation in freestanding semiconductor NWs through the direct injection of holes and electrons without the need for plasmonic coupling. Spectra obtained in this manner closely resemble the corresponding PL spectra. Even though no direct correlation between the luminescent areas and the STM topography could be observed, the light emission of CdSe NWs was found to be governed by diameter-dependent quantum size effects in the zinc blende-type wire sections. Future STL-based studies could enable the combination of topography imaging with local light emission and tunneling spectroscopy on semiconductor NWs.

## 4. Experimental Section

The NWs were grown by the SLS method using Bi nanoparticle catalysts, as detailed in Reference [43]. Subsequently, the wires were dispersed in chloroform by ultrasonication, and then

deposited by spin-coating onto a clean substrate under ambient conditions. The substrates consisted of a 55-nm-thick gold film evaporated onto a Si substrate with a 300-nm-thick, thermally grown $SiO_2$ layer. The diameters of the wires investigated in the STM experiments ranged between 7 and 22 nm. Prior to STM measurements, atomic force microscopy (AFM) was employed to determine the density of the NWs on the substrate. The AFM images confirmed that most of the NWs were separate from each other without forming bundles. Electrochemically etched tungsten tips were used as STM tips. The experimental setup for the detection of STM-induced luminescence is described in detail elsewhere.[17] Briefly, photons originating from the tunneling junction (Figure 1a) were collected by an aspheric lens of numerical aperture 0.42 in close proximity to the tip. The emitted light was spectrally analyzed by an Acton Research Spectra Pro 300i spectrograph equipped with a 150 lines per inch blazed grating and a Peltier-cooled CCD camera behind a light intensifier. Photon intensity maps were recorded using a Perkin–Elmer silicon avalanche photodiode (SPCM-AQRH-15) specified with 50 dark counts per second. The PL measurements were performed at 12 K in a different setup using a confocal laser-scanning microscope. For an excitation wavelength of 532 nm and a microscope objective of numerical aperture 0.7, a spatial resolution of approximately 500 nm was reached.

[1] X. Duan, Y. Huang, Y. Cui, J. Wang, C. M. Lieber, *Nature* **2001**, *409*, 66.
[2] J. K. Gimzewski, B. Reihl, J. H. Coombs, R. R. Schlittler, *Z. Phys. B* **1988**, *72*, 497.
[3] D. L. Abraham, A. Veider, C. Schönenberger, H. P. Meier, D. J. Arent, S. F. Alvarado, *Appl. Phys. Lett.* **1990**, *56*, 1564.
[4] T. Tsuruoka, Y. Ohizumi, R. Tanimoto, S. Ushioda, *Appl. Phys. Lett.* **1999**, *75*, 2289.
[5] M. Kemerink, J. W. Gerritsen, P. M. Koenraad, H. van Kempen, J. H. Wolter, *Appl. Phys. Lett.* **1999**, *75*, 3656.
[6] L. Samuelson, A. Gustafsson, J. Lindahl, L. Montelius, M. E. Pistol, J. O. Malm, G. Vermeire, P. Demeester, *J. Vac. Sci. Technol. B* **1994**, *12*, 2521.
[7] M. Pfister, M. B. Johnson, S. F. Alvarado, H. W. M. Salemink, U. Marti, D. Martin, F. Morier-Genoud, F. K. Reinhart, *Appl. Phys. Lett.* **1994**, *65*, 1168.
[8] S. E. J. Jacobs, M. Kemerink, P. M. Koenraad, M. Hopkinson, H. W. M. Salemink, J. H. Wolter, *Appl. Phys. Lett.* **2003**, *83*, 290.
[9] U. Hakanson, H. Hakanson, M. K. J. Johansson, L. Samuelson, M. E. Pistol, *J. Vac. Sci. Technol. B* **2003**, *21*, 2344.
[10] T. Tsuruoka, Y. Ohizumi, S. Ushioda, *J. Appl. Phys.* **2004**, *95*, 1064.
[11] M. J. Romero, J. van de Lagemaat, I. Mora-Sero, G. Rumbles, M. M. Al-Jassim, *Nano Lett.* **2006**, *6*, 2833.
[12] M. J. Romero, J. van de Lagemaat, *Phys. Rev. B* **2009**, *80*, 115432.
[13] A. J. Mäkinen, E. E. Foos, J. Wilkinson, J. P. Long, *J. Phys. Chem. C* **2007**, *111*, 8188.
[14] R. Berndt, J. K. Gimzewski, P. Johansson, *Phys. Rev. Lett.* **1991**, *67*, 3796.
[15] G. Hoffmann, J. Aizpurua, P. Apell, R. Berndt, *Surf. Sci.* **2001**, *482–485*, 1159.
[16] Ö. Kurtulus, Z. Li, A. Mews, U. Pietsch, *Phys. Status Solidi A* **2009**, *206*, 1752.
[17] K. Kuhnke, A. Kabakchiev, W. Stiepany, F. Zinser, R. Vogelgesang, K. Kern, *Rev. Sci. Instrum.* **2010**, *81* 113102.
[18] R. Berndt, J. K. Gimzewski, *Surf. Sci.* **1992**, *269–270*, 556.
[19] M. S. Gudiksen, K. N. Maher, L. Ouyang, H. Park, *Nano Lett.* **2005**, *5*, 2257.
[20] Y.-J. Doh, K. N. Maher, L. Ouyang, C. L. Yu, H. Park, J. Park, *Nano Lett.* **2008**, *8*, 4552.
[21] S. Adachi, *Handbook on Physical Properties of Semiconductors*, Vol. 3, Kluwer Academic, Dordrecht **2004**.
[22] V. V. Protasenko, K. L. Hull, M. Kuno, *Adv. Mater.* **2005**, *17*, 2942.
[23] M. S. Gudiksen, J. Wang, C. M. Lieber, *J. Phys. Chem. B* **2002**, *106*, 4036.
[24] H. Yu, J. Li, R. A. Loomis, P. C. Gibbons, L.-W. Wang, W. E. Buhro, *J. Am. Chem. Soc.* **2003**, *125*, 16168.
[25] F. Wang, H. Yu, S. Jeong, J. M. Pietryga, J. A. Hollingsworth, P. C. Gibbons, W. E. Buhro, *ACS Nano* **2008**, *2*, 1903.
[26] S. Alvarado, P. Renaud, H. Meier, *J. Phys. IV* **1991**, *1*, 271.
[27] H. Yu, J. Li, R. A. Loomis, L.-W. Wang, W. E. Buhro, *Nat. Mater.* **2003**, *2*, 517.
[28] R. Berndt, J. K. Gimzewski, P. Johansson, *Phys. Rev. Lett.* **1993**, *71*, 3493.
[29] P. Johansson, *Phys. Rev. B* **1998**, *58*, 10823.
[30] D. G. Walmsley, T.-S. Tan, P. Dawson, *Surf. Sci.* **2004**, *572*, 497.
[31] A. Lan, J. Giblin, V. Protasenko, M. Kuno, *Appl. Phys. Lett.* **2008**, *92*, 183110.
[32] R. Berndt, J. K. Gimzewski, *Phys. Rev. B* **1992**, *45*, 14095.
[33] M. Wenderoth, M. J. Gregor, R. G. Ulbrich, *Solid State Commun.* **1992**, *83*, 535.
[34] V. Snejdar, J. Jerhot, *Thin Solid Films* **1972**, *11*, 289.
[35] A. Kurokawa, J. Muto, *J. Mater. Sci.: Mater. Electron.* **2003**, *14*, 33.
[36] N. G. Dhere, N. R. Parikh, A. Ferreira, *Thin Solid Films* **1977**, *44*, 83.
[37] H.-J. Choi, J.-K. Yang, J.-H. Park, *Thin Solid Films* **2006**, *494*, 207.
[38] L. Zhang, J.-W. Luo, A. Zunger, N. Akopian, V. Zwiller, J.-C. Harmand, *Nano Lett.* **2010**, *10*, 4055.
[39] R. Zhou, H.-C. Chang, V. Protasenko, M. Kuno, A. K. Singh, D. Jena, H. Xing, *J. Appl. Phys.* **2007**, *101*, 073704.
[40] L.-S. Li, A. P. Alivisatos, *Phys. Rev. Lett.* **2003**, *90*, 097402.
[41] T. Nann, J. Schneider, *Chem. Phys. Lett.* **2004**, *384*, 150.
[42] L. M. Smith, H. E. Jackson, J. M. Yarrison-Rice, C. Jagadish, *Semicond. Sci. Technol.* **2010**, *25*, 024010.
[43] Z. Li, A. Kornowski, A. Myalitsin, A. Mews, *Small* **2008**, *4*, 1698.